Available online at BCREC website: https://bcrec.id

Bulletin of Chemical Reaction Engineering & Catalysis, 18 (3) 2023, 521-538

Research Article

An Experimental and Computational Study of Zeolitic Imidazolate Framework (ZIF-8) Synthesis Modulated with Sodium Chloride and Its Interaction with CO_2

Lita Priandani[1], Amarilis Aliefa[1], Oka Pradipta Arjasa[2], Fajar Inggit Pambudi[1,*]

[1]Department of Chemistry, Faculty of Mathematics and Natural Sciences, Universitas Gadjah Mada, Sekip Utara Bulaksumur Yogyakarta 55281, Indonesia.
[2]Advanced Materials Research Centre - National Research and Innovation Agency, Banten 15314, Indonesia.

Received: 6th September 2023; Revised: 3rd October 2023; Accepted: 3rd October 2023
Available online: 9th October 2022; Published regularly: October 2023

Abstract

The increase of CO_2 level in atmosphere becomes one of the driving forces for research on functional materials. Capturing and utilizing of CO_2 are more important than ever, both to reduce CO_2 emission and to increase the economic value of CO_2 derivatives. In this study, synthesis of metal-organic frameworks (MOFs) was conducted by combining Zn^{2+} metal nodes and 2-methylimidazolate ligand to form zeolitic imidazolate frameworks (ZIF-8) materials. ZIF-8 was synthesised with the addition of sodium chloride to modulate the crystal morphology during the in-situ synthesis, using either water or methanol as the solvent. According to the refinement of the X-ray diffraction pattern, the ZIF-8 materials were successfully prepared and have unit cell parameters that are reasonably close to the available standard. The formation of ZIF-8 is also confirmed by IR spectroscopy, which reveals the stretching vibration mode of Zn−N from the coordination between Zn^{2+} and 2-methylimidazolate ligand. The crystal morphology exhibits different shape, as observed in SEM and TEM studies, with the dominant shape being a rhombic dodecahedron. The interaction between ZIF-8 and CO_2 was investigated via ex-situ IR spectroscopy, combined with several computational techniques such as density functional theory and molecular dynamics, to elucidate the nature of the CO_2 binding sites.

Keywords: ZIF-8; synthesis; structure; carbon dioxide; DFT; crystal morphology

How to Cite: L. Priandani, A. Aliefa, O.P. Arjasa, F.I. Pambudi (2023). An Experimental and Computational Study of Zeolitic Imidazolate Framework (ZIF-8) Synthesis Modulated with Sodium Chloride and Its Interaction with CO_2. *Bulletin of Chemical Reaction Engineering & Catalysis*, 18(3), 521-538 (doi: 10.9767/bcrec.20033)

Permalink/DOI: https://doi.org/10.9767/bcrec.20033

1. Introduction

The presence of carbon dioxide (CO_2) in atmosphere can be challenging when its concentration is far beyond the acceptable threshold [1,2]. Capturing and utilizing CO_2 therefore become important strategy to reduce the emission of CO_2 in atmosphere [3,4]. Transforming CO_2 into some valuable chemical is one of the main goals of capturing CO_2. Functional materials have been reported which act as catalyst to transform CO_2 [5–7]. However, utilizing CO_2 may require an effective strategy to capture CO_2 gas. One of which is using functional materials which can bind selectively towards CO_2 but it is expected to release CO_2 easily. To this end, functional materials, such as metal-organic frameworks (MOFs), have emerged to become an effective and selective adsorbent to capture as well as act as catalyst to transform CO_2 gas [8–10].

* Corresponding Author.
Email: fajar.inggit@ugm.ac.id (F.I. Pambudi)

MOFs as functional materials consist of metal nodes or cluster and organic linkers to give a periodic structure or framework which has a defined size of cages or pores [11,12]. MOFs can be finetuned to modify the crystal properties such as the morphology and the functional sites that are present inside the MOFs pore. Therefore, the use of MOFs for CO_2 capture is possible by modifying the nature of the MOFs framework [13]. Several MOFs have been reported as material to capture CO_2, such as MIL-96 [14], MIL-102 [15], ZIF-100 [16], $Zn_2(ndc)_2(dpni)$ [17], $Zn_2(cnc)_2(dpt)$ [18], MIL-53 [19], PCN-5 [20], and ZIF-20 [21].

An example of MOFs is zeolitic imidazolate framework-8 (ZIF-8). ZIF-8 consists of Zn^{2+} ion as the metal nodes connected with four 2-methylimidazolate ligands forming a tetrahedral geometry which then form a 3D periodic structure. ZIF-8 has large sodalite cages which are accessible for the diffusion of CO_2 molecules. ZIF-8 has been reported to have relatively high stability compared to other MOFs, therefore it might be suitable for application where humidity is high. Modification of ZIF-8 is also possible by inducing different type of metal ions doping to give mixed-metal ZIF such as ZIF-8 containing, Ni, Fe, Cu, Co and Cd [22–24]. Further modification of ZIF-8 is also possible by introducing different organic linkers, such as 2-aminobenzimidazole and 2-ethylimidazole [25,26].

The synthesis of MOFs can be further modulated by adding some chemicals which are not the main backbone of the MOF structure. Several examples of modulating agents are surfactant (cetyltrimethylammonium bromide), triethylamine, pyridine, polyvinylpyrrolidone, inorganic salts *etc*. [27–31]. In this report, the synthesis of ZIF-8 crystals was studied by the addition of inorganic salt particularly sodium chloride (NaCl) using different solvents such as methanol and water-based system. The use of different solvents in the presence of inorganic salt has not been thoroughly studied in the previous studies in term of ZIF-8 synthesis. Furthermore, the use of two different solvents of either water or methanol was assessed to examine the effect of solvent on the crystal morphology and possible interaction with CO_2 molecule. Therefore, it is expected that the presence of NaCl inside the ZIF-8 sodalite cage will provide more binding sites for the attachment of CO_2 molecules. Additionally, characterizations using density functional theory (DFT) as well as molecular dynamics were conducted to unravel the nature of CO_2 interaction with ZIF-8 modulated NaCl in the presence of either water or methanol solvent. Therefore, a thorough study on the effect of solvent and inorganic salt during interaction with CO_2 is provided to give an in-depth study of host-guest system in ZIF-8 material.

2. Materials and Methods

2.1 Materials

The chemicals of $Zn(NO_3)_2.6H_2O$ (Sigma Aldrich, 98%), 2-methylimidazole (Sigma Aldrich 99%), sodium chloride (Merck), methanol, distilled water, and acetone were used without further purification.

2.2 Synthesis of ZIF-8

A typical synthesis of ZIF-8 was conducted using the specific ratio of $Zn(NO_3)_2.6H_2O$ and 2-methylimidazole. Pristine ZIF-8 was synthesised by dissolving 0.148 g of $Zn(NO_3)_2.6H_2O$ in 2 mL of distilled water to give solution 1. The organic linker of 2-methylimidazole (2.463 g) was dissolved in 18 mL distilled water to give solution 2. Solution 1 and 2 were mixed in a glass vial and stirred for 10 min at room temperature. The mixture was left at room temperature for 24 h. The precipitates of ZIF-8 crystals were vacuum filtered using a sinter funnel. The solid products were dried in an oven at 60 °C for 12 h. The same pristine ZIF-8 crystals were also made by using methanol as the solvent. The crystals were then characterized by powder X-ray diffraction method at 2θ of 5–50° using Cu-Kα (λ = 1.54060 Å) radiation. Scanning electron microscope and transmission electron microscope were also used to identify the crystal morphology. Fourier transform IR spectroscopy was also used to examine the solid ZIF-8 product.

2.3 Synthesis of NaCl@ZIF-8

The same method to synthesis ZIF-8 is used for making NaCl@ZIF-8. In a typical synthesis, $Zn(NO_3)_2.6H_2O$ and 2-methylimidazole were mixed in a glass vial with the addition of either H_2O or methanol as the solvent. Into the mixture, NaCl were added with the following quantities of 0.25, 0.50, 1.00, and 1.50 mmol for water solvent and 0.3, 0.7, 1.0, and 2.0 mmol for methanol solvent.

2.4 Ex-situ IR Spectroscopy Study of CO_2 Adsorption

The pristine ZIF-8 was washed several times and heated at 60 °C for 12 h to reduce the solvent contents inside the ZIF-8 pore. The

ZIF-8 sample (2.2 mg) was then placed in a 20 mL glass vial. The glass vial was tightly closed while CO_2 gas was injected through a syringe with a flow rate of maximum 100 mL/min for 5 min. This is to ensure that the CO_2 concentration was saturated inside the glass vial. After the adsorption experiment, the sample was analyzed using an ex-situ IR spectroscopy. The same treatment was also performed for ZIF-8 doped with NaCl.

2.5 Computational Methods

Density Functional Theory (DFT) studies were conducted by using Orca 5.0.3 [32]. The calculations were performed to unveil the interactions between ZIF-8 and NaCl as well as the presence of solvent and CO_2. Following our previous work, the ZIF-8 structure was simplified from the periodic structure to give a cluster of Zn^{2+} ion connected to four 2-methylimidazolate ligands [33]. The 2-methylimidazolate ligands were capped with hydrogen as shown in Figure 1(a). To maintain the tetrahedral geometry of ZIF-8 cluster, the capping atoms of hydrogen were constrained during all calculations. The calculations were conducted using the generalized gradient approximation with Perdew-Burke-Ernherzof functional [34]. The convergence criteria were set to the default of Orca 5.0.3 with a tight SCF. Basis set of def2-tzvp was used for all atoms. Dispersion correction scheme of D3BJ was used to accommodate possible weak interactions [35]. Additional calculation at the periodic ZIF-8 structure (Figure 1(b)) was also performed using the GFN2-xTB method implemented in the DFTB+ package to follow the CO_2 molecular dynamics within the ZIF-8 cage [36,37]. A periodic ZIF-8 containing six molecules of either water or methanol as solvent was built with the addition of NaCl and H_2O. The temperature was maintained at 298 K by using Nose Hoover thermostat. The timestep of the integration motion was set at 0.5 fs. A total of 10 ps simulation time was used and the trajectory was kept every 10 fs. The last 1500 frames of the trajectory file were used to analyse ZIF-8 structure.

3. Results and Discussion

3.1 Synthesis and Characterization of ZIF-8

Synthesis of pristine ZIF-8 has been successfully conducted when either water or methanol were used as the primary solvent. According to the powder X-ray diffraction pattern, the water-based solvent of pristine ZIF-8 shows several main peaks similar to the reported literature as shown in Figure 2 [38]. The same X-ray diffraction pattern was also observed for ZIF-8 synthesised using methanol as the solvent. Analysis using the Le Bail fit method resulted in lattice parameter of a = 16.9758 Å and a = 16.9869 Å for ZIF-8 made with water and methanol, respectively. All powder X-ray diffraction data were refined with cubic crystal system and a space group of I−43m following

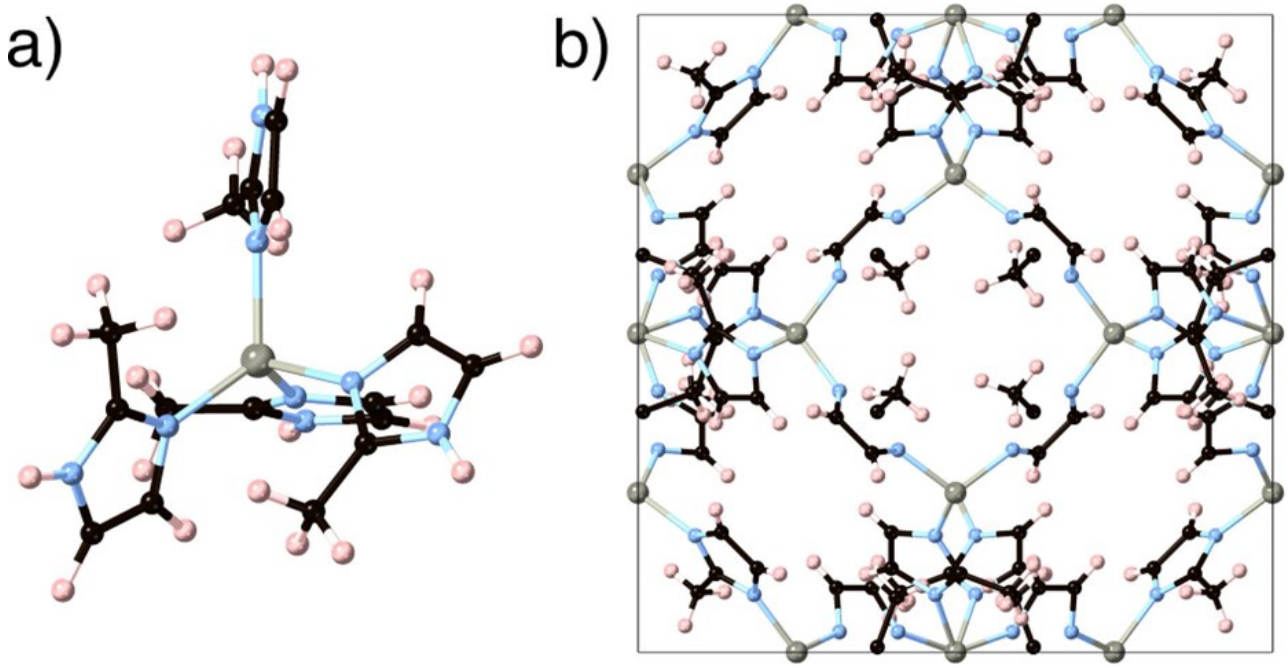

Figure 1. $Zn(2\text{-MeIM})_4$ cluster (a) and periodic structure of ZIF-8 shown from (100) facet. Zn, C, N and H are coloured grey, black, cyan and pink, respectively.

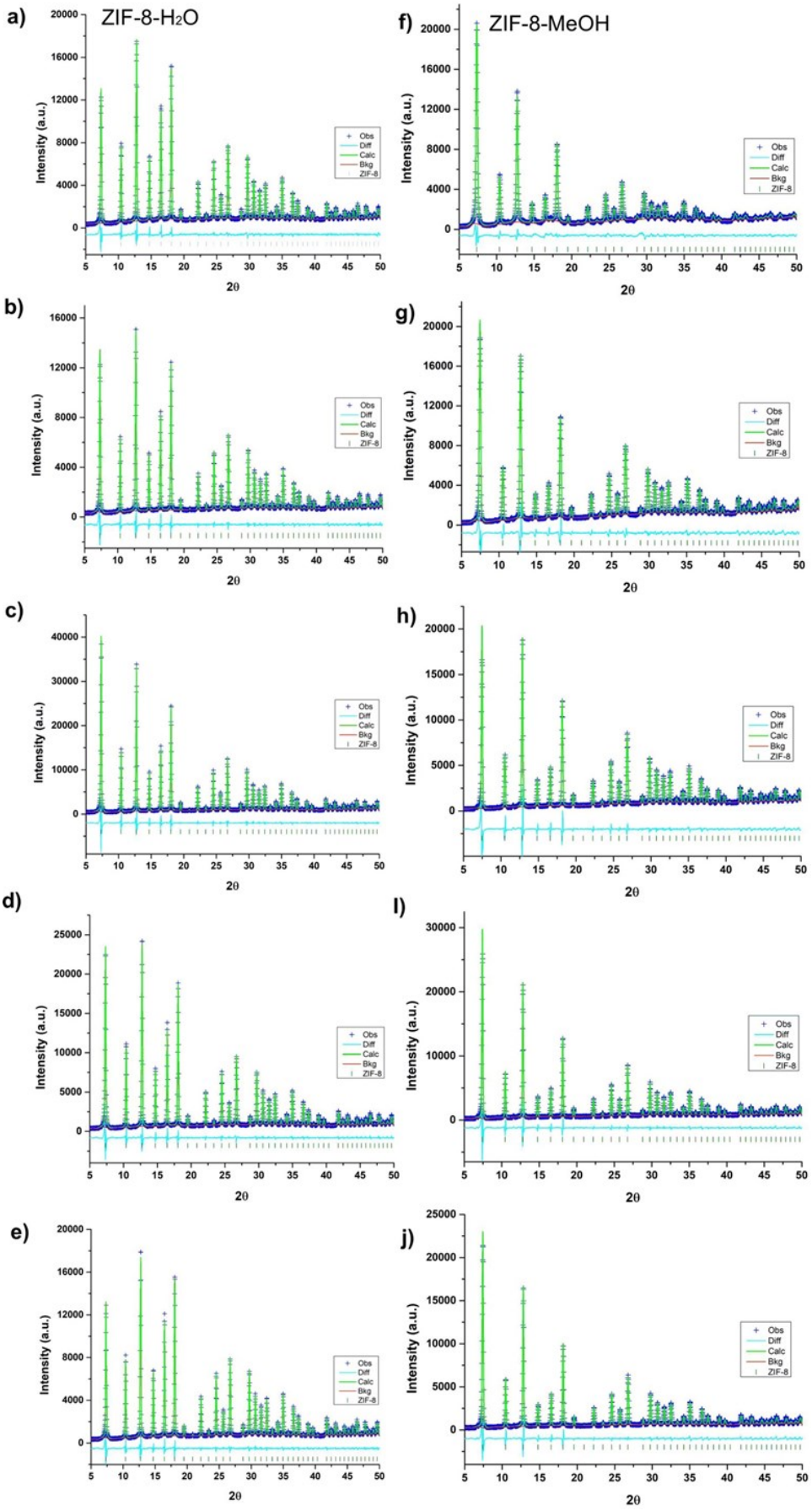

Figure 2. Powder X-ray diffraction pattern of pristine ZIF-8 synthesised with water (a) and methanol (f). Modulated ZIF-8 with NaCl is also shown for water (b-e) and methanol (g-j).

the reported structure with CCDC number of 602542. Looking at the different solvents, the crystallinity of ZIF-8 made with water solvent has generally lower intensity especially at 2θ of ~7.3°. This is corresponding to the {110} lattice planes of the ZIF-8 crystals with d_{110}-spacing of 12.003 Å and 12.013 Å for crystals with water and methanol-based solvent, respectively. The significant occurrence of {110} planes predict the dominance crystal surface morphology with this {110} facet. Different observation is observed for 2θ of ~8.49° indicating the {200} lat-

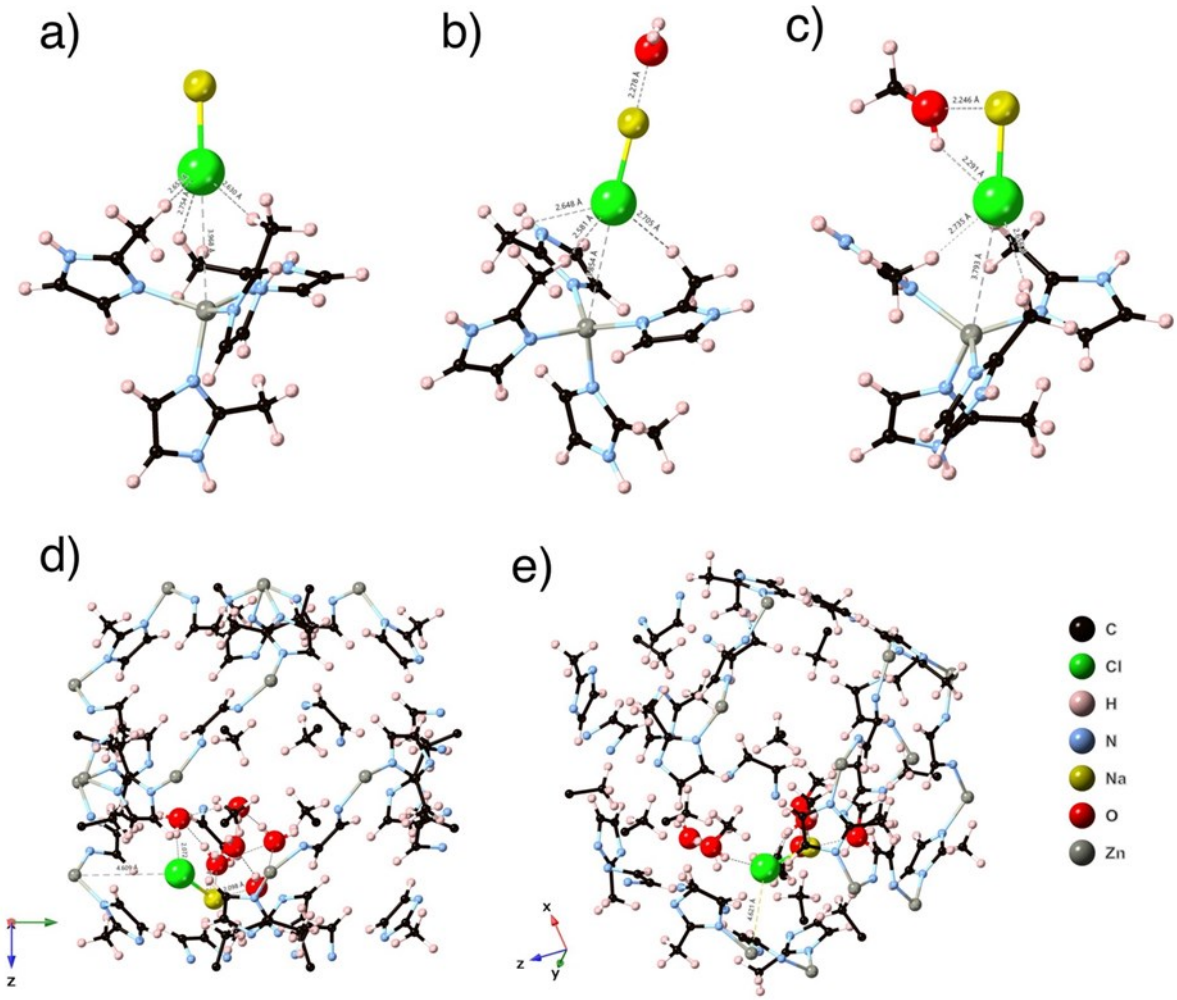

Figure 3. The optimized geometries of NaCl@ZIF-8 cluster (a), NaCl@ZIF-8 cluster interacting with H_2O (b) and methanol (c), and periodic structure of ZIF-8 containing NaCl with H_2O (d) and methanol (e) clusters.

Table 1. The lattice parameter of ZIF-8 synthesised using water and methanol as well as in the presence of NaCl.

No	Samples	*a*-lattice	Space group	R_w
1	ZIF-8-H2O	16.9758(2)	I$\bar{4}$3m	6.43
2	ZIF-8-MeOH	16.9869(6)	I$\bar{4}$3m	6.54
3	ZIF-8-MeOH-NaCl-0.3	16.9913(5)	I$\bar{4}$3m	9.26
4	ZIF-8-MeOH-NaCl-0.7	17.0088(5)	I$\bar{4}$3m	12.89
5	ZIF-8-MeOH-NaCl-1.0	16.9967(4)	I$\bar{4}$3m	11.56
6	ZIF-8-MeOH-NaCl-2.0	16.9918(4)	I$\bar{4}$3m	9.96
7	ZIF-8-H_2O-NaCl-0.25	17.0229(2)	I$\bar{4}$3m	7.22
8	ZIF-8-H_2O-NaCl-0.5	17.000(1)	I$\bar{4}$3m	9.35
9	ZIF-8-H_2O-NaCl-1.0	17.0211(2)	I$\bar{4}$3m	7.64
10	ZIF-8-H_2O-NaCl-1.5	17.0215(2)	I$\bar{4}$3m	6.10

tice planes. The relative intensity of {200} planes in ZIF-8 made with water is higher than it in ZIF-8 synthesised with methanol. The d_{200} spacing is calculated to be 8.487 Å and 8.493 Å for ZIF-8 crystals made with water and methanol, respectively. This d_{200} spacing is actually the half of the unit cell dimension of *a* with lattice planes family of {100}. This {100} planes are corresponding to the eight crystal surfaces of cubic system. Therefore, the nature of the crystal shape can be predicted based on the powder X-ray diffraction pattern for ZIF-8 synthesised using water (Figure 2(a)) and methanol (Figure 2(f)).

The presence of NaCl as the doping agent has less effect to the structural arrangement of ZIF-8 structure. The powder X-ray diffraction patterns indicates no additional crystal phase since all the peaks are able to be assigned as ZIF-8 crystal phase. In addition, there is no significant shift of the d-spacing due to the presence of NaCl. However, slightly difference of lattice parameter is observed compared to the pristine ZIF-8. The summary of the lattice parameter obtained from the Le bail fit method is given in Table 1.

The presence of NaCl inside the ZIF-8 structure resulted in small deviation of *a*-lattice parameter as given in Table 1. However, this deviation is relatively small compared to the reported lattice parameter. ZIF-8 has been reported to be synthesized in N,N-dimethylformamide solvent to give single crystal form with lattice parameter of 16.9910 Å [38]. This value is relatively similar to the lattice parameter of ZIF-8 doped with NaCl. Therefore, NaCl is predicted to be inserted inside the ZIF-8 pore without occurring ion exchange with Zn^{2+} ions.

DFT calculations were performed to unveil the possible interaction between NaCl and ZIF-8. The ZIF-8 structure was modelled by cutting the periodic structure to give a cluster model of $Zn(2\text{-MeIM})_4$ as shown in Figure 3(a-c). The NaCl was positioned relatively close to the Zn^{2+} ions and allowed to relax. To confirm the nature of NaCl inside ZIF-8 pore, periodic structure calculation was performed by implementing GFN2-xTB method. By using this method, it is possible to calculate the optimized structure for the whole unit cell of ZIF-8 containing NaCl and solvent molecule as shown in Figure 3(d-e).

The presence of methanol in the ZIF-8 cages slightly affect the unit cell dimensions with the value of a = 16.9869 Å. This value is 0.06% bigger than the unit cell in water-based solvent. This slightly big unit cell can be explained due to the nature of larger molecular size of methanol than water molecule. In Figure 3(e), the interaction between methanol and ZIF-8 is modelled. It shows that the location of methanol molecule is distributed in larger space than water solvent (Figure 3(d)). The interaction between methanol molecules occupy relatively large ZIF-8 cages due to the hydrogen bonding between two methanol molecules, where the methyl group (CH_3–OH) points in different orientations. An isolated model of methanol cluster in the presence of NaCl is given in Figure S1. In this case, the presence of NaCl is also affecting the methanol–methanol interaction. Consequently, the calculated unit cell provides slightly larger unit cell than it in water based solvent.

The position of NaCl is relatively close to the methyl group of the 2-methylimidazolate ligand with approximate distance of 2.754 Å as seen in Figure 3(a). Therefore, the presence of NaCl is also affecting the unit cell slightly compared to the pristine ZIF-8 either in methanol or water solvents. In this position, Cl^- has the closest distance to the Zn^{2+} ion with a distance of 3.968 Å indicating possible intermolecular interaction between Cl^- and Zn^{2+} in the form of electrostatic interaction. From the X-ray diffraction pattern in Figure 2, the structure of ZIF-8 seems to be less affected by the presence of NaCl inside the pore, therefore there is a possibility that NaCl resides within ZIF-8 pore through possible intermolecular interaction. To confirm this intermolecular interaction, independent gradient model (IGM) was used to check the type of intermolecular that might present. As shown in Figure S2, the interaction between NaCl and ZIF-8 cluster is dominated by van der Walls interaction as well as attracting interaction such as electrostatic attraction. Looking at the Na^+, Cl^- and Zn^{2+} radii, the ionic radius of Na^+ (116 pm) and Cl^- (181 pm) are bigger than it in Zn^{2+} ion with 88 pm. Due to large ionic radius difference, the possibility of Na^+ to replace Zn^{2+} in the ZIF-8 frameworks is low. The presence of solvent molecule is also predicted to be relatively close to the Na^+ and Cl^- ions as shown in Figure 3(b) and 3(c). As expected, water molecule will have close interaction with Na^+ ion through O atom with approximate distance of 2.278 Å. The same behaviour is also observed for the methanol solvent where the O and H of CH_3–OH are relatively close to the Na^+ and Cl^- with a distance of 2.246 Å and 2.291 Å, respectively.

The interaction between NaCl and periodic structure of ZIF-8 was also conducted in the presence of solvent cluster of either H_2O or

methanol as shown in Figure 3(d-e). The Na^+ and Cl^- were place inside the pore together with six solvent molecules of water or methanol and allowed to relax. Similar with the DFT calculation of $Zn(2\text{-MeIM})_4$ cluster, the Cl^- is relatively close to the Zn^{2+} sites with a distance of 4.609 Å and 4.621 Å when water and methanol were used as the solvent, respectively. The behaviour of water molecules indicates an expected interaction where hydrogen bonding between water molecules are presence to give water cluster that is close to the Na^+ and Cl^-. Water molecules are predicted to interact with 2-methylimidazolate ligand with an average distance of 3.237 Å to C atom. The same observation is also shown for methanol cluster, where the O atom (−OH) is relatively close to the Na^+ ions in addition to the interaction between methanol and 2-methylimidazolate ligand.

Characterization based on the IR spectroscopy was conducted to check the formation of ZIF-8 crystal. In Figure 4, the IR spectra of initial reagents, pristine ZIF-8 and ZIF-8 doped with NaCl are shown. The IR spectrum of $Zn(NO_3)_2.6H_2O$ and 2-methylimidazolate shows characteristic peaks that are combined into ZIF-8 crystals. A new peak at 421 cm^{-1} appears due to the interaction between Zn^{2+} ion and N of 2-methylimidazolate ligand to give Zn−N stretching vibration. This shows the formation of coordination interaction between Zn^{2+} and four 2-methylimidazolate ligands. The small peak at around 3200 cm^{-1} might indicates the vibration from N−H of the 2-methylimidazol ligand. However, this peak disappears when the proton of the 2-methylimidazole is replaced by Zn^{2+} ion to give ZIF-8. The contribution from the 2-methylimidazolate ligand vibration is significant in the fingerprint region. The peak at 1577 cm^{-1} might indicate the stretching vibration of C=N while the peak at around 1145 cm^{-1} shows possible stretching vibration from the weaker bond of C−N. The 2-methylimidazolate ligand also has stretching vibration from the aromatic ring that can be identified from 1307 cm^{-1} to 1457 cm^{-1}. In addition, the stretching vibration from Csp_3−H of the methyl group in 2-methylimidazolate can be observed at higher wavenumber of 2926 cm^{-1}. At wavenumber of approximately 3200 cm^{-1} to 3500 cm^{-1}, a slightly wide peak can be observed which can be identified as possible vibration from solvent molecules due to O−H vibration of either water or methanol clusters. The same observation present in both ZIF-8 synthesised using water and methanol.

To confirm the formation of ZIF-8 modulated with NaCl, we have performed frequency analysis on the model of ZIF-8 cluster capped with NaCl as shown in Figure 3(a). The calculation shows that various vibration due to the presence of 2-methylimidazolate ligand occur which is approximately similar to the experimental results. A characteristic of Zn–N vibration can be observed at 375 cm^{-1} form the DFT calculation based on PBE functional. This indicates that the calculated spectra have reasonably close to the experimental data confirming the formation of polymeric Zn−N bond to give ZIF-8 crystals.

The crystal morphology of ZIF-8 doped with NaCl has been characterized using both SEM and TEM for selected samples. In Figure 5, the SEM images of ZIF-8 and ZIF-8 doped with NaCl are given. All the SEM images show a scale bar of 1 μm for the ease of comparing. As seen for pristine ZIF-8 made with either water or methanol, the crystal shape is relatively homogenous with approximately spherical shape. And it is also shown in the SEM image of both

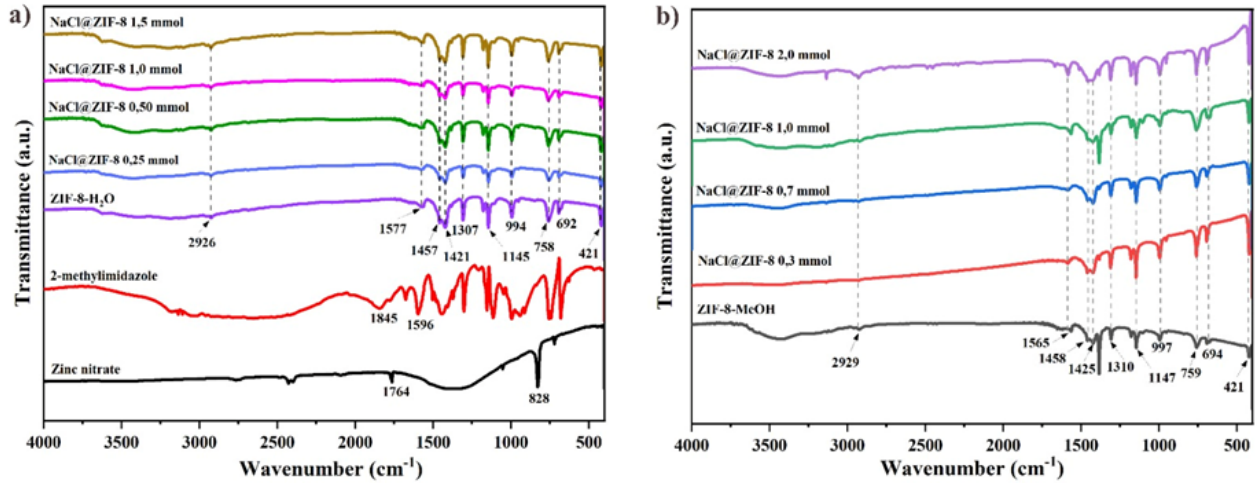

Figure 4. IR spectra of ZIF-8 synthesised in water (left) and methanol (right).

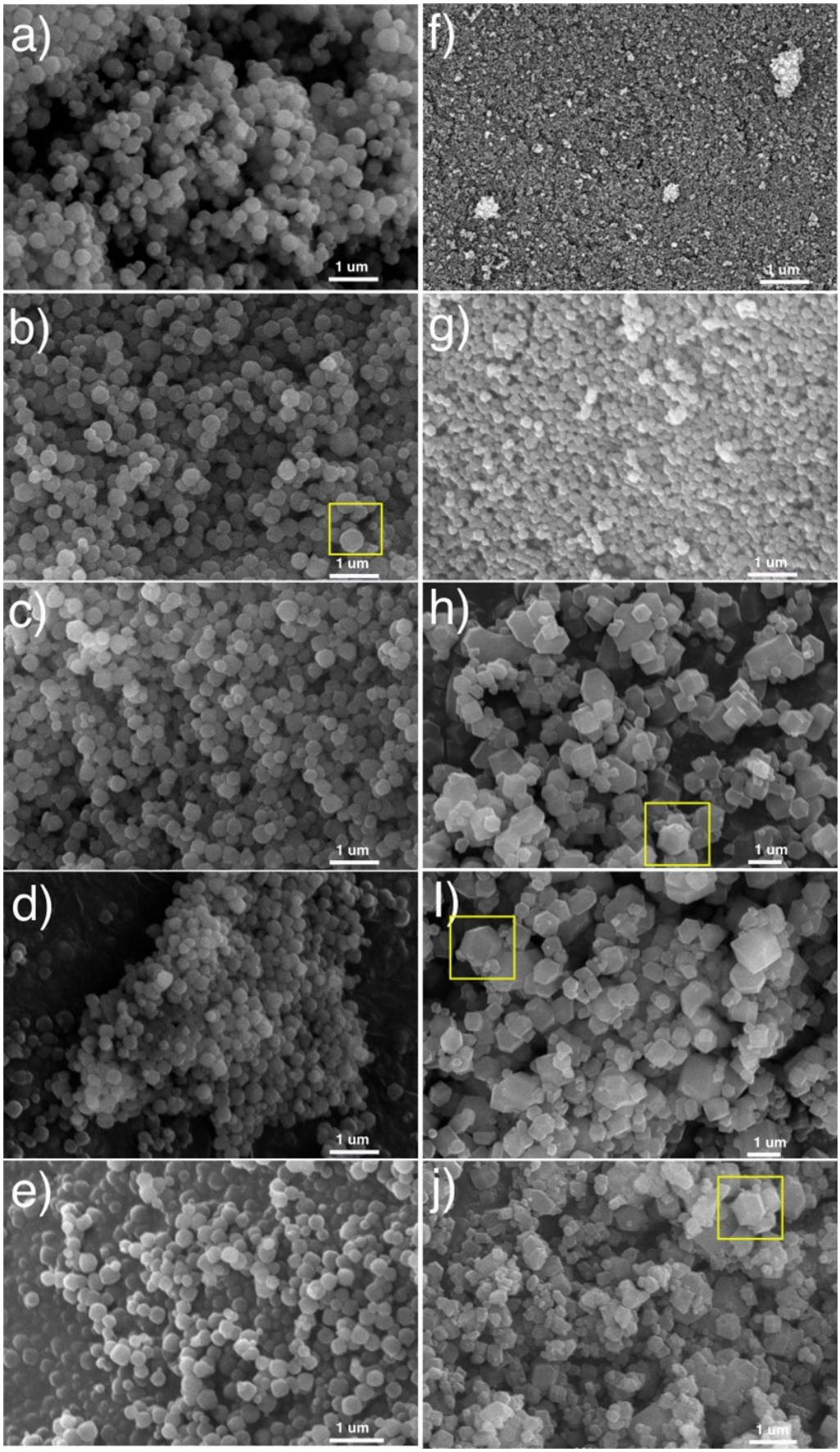

Figure 5. SEM images of pristine ZIF-8 synthesised in water (a) and methanol (f). ZIF-8 crystal doped with NaCl synthesised using water (b-e) and methanol (g-j) were also shown. Scale bar in the SEM images is 1 μm for all images.

materials that the average particle size is about 300 nm and 74.2 nm for ZIF-8 made with water and methanol, respectively (see Figure S3 and S4 for the particle size distribution). When pristine ZIF-8 was added with NaCl during the in-situ synthesis, the particle size remains relatively the same for ZIF-8 doped with NaCl under water solvent as shown in Figure 5(b-e). The particle size still indicates approximately 300 nm in diameter with spherical shape. However, several ZIF-8 particles can be identified to have relatively clear crystal facet as shown in the yellow rectangular in Figure 5(b).

ZIF-8 doped with NaCl under methanol solvent shows different behaviour compared with water-based synthesis. Although the particle size of pristine ZIF-8 under methanol is smaller than ZIF-8 under water solvent, increasing the content of NaCl raises the particle size to 213 nm in average for ZIF-8 modulated with 0.3 mmol NaCl (Figure 5(g)). The particle size is generally increasing when more NaCl is added during the in-situ synthesis. In addition, the crystal shape of ZIF-8 become apparent when methanol solvent was used during the synthesis. In Figure 5(h-j), the yellow rectangular shows ZIF-8 particle which have clear crystal facet showing possible {110} crystal facets. Comparing with available literatures, the crystal shape of ZIF-8 under methanol solvent shows a rhombic dodecahedron shape where the dominant crystal facets occur for the family of {110} facets. This is also corresponding to the X-ray diffraction pattern where the lattice planes of {110} family have relatively high intensity as shown in Figure 2.

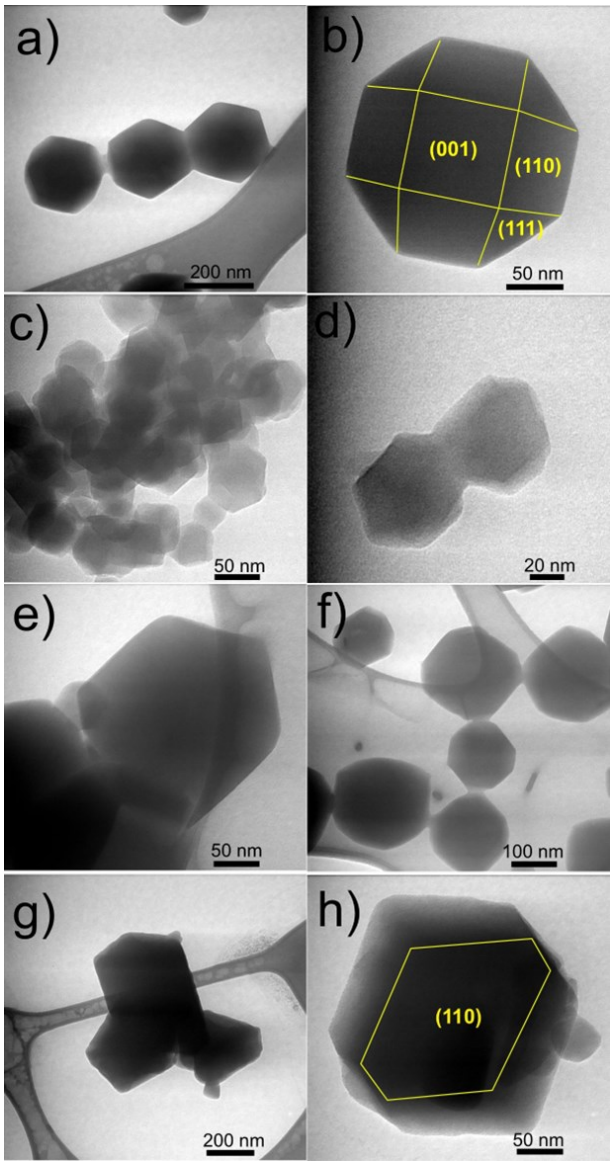

Figure 6. TEM images of pristine ZIF-8 synthesised with water (a,b) and methanol (c,d) as well as ZIF-8 doped with NaCl under water (e,f) and methanol (g,h) solvent.

To confirm the nature of ZIF-8 crystals, TEM images are provided in Figure 6 showing different particle size and crystal shape. Pristine ZIF-8 made with water solvent exhibits relatively big crystal with crystal size of approximately 100 nm to 200 nm. This crystal size is relatively bigger than ZIF-8 obtained from methanol solvent with size of ~50 nm. This is reasonably similar with the observation from the SEM images. The presence of NaCl during the in-situ synthesis of ZIF-8 affects the crystal size for ZIF-8 made with methanol solvent but less when water was used during the synthesis. ZIF-8 doped with NaCl under methanol solvent has larger crystal size of approximately ~200 nm than without doping with NaCl.

The difference in crystal size can be predicted due to the nature of interaction between methanol or water molecule and ZIF-8 structure. As shown in Figure 3(b) and 3(c), the water molecule has relatively strong interaction with NaCl but less with the 2-methylimidazolate ligand with the closest approximate distance of 6.491 Å. However, methanol molecule is predicted to have the same interaction with NaCl but has closer interaction to the 2-methylimidazolate ligand with the closest distance is approximately 3.259 Å. Therefore, the presence of methanol with larger molecular dimension than water molecule affects the nucleation and crystal growth process by hindering the interaction between Zn^{2+} and 2-methylimidazolate ligand. The rate of nucleation is predicted to be lower when methanol is present to give relatively bigger crystal size.

The crystal facets revealed from the TEM images indicate a characteristic surface of cubic structure of ZIF-8 crystals. In pristine ZIF-8 made with water solvent, the characteristic of possible truncated cubic shape is shown in Figure 6(b). The truncated cubic indicates dominant crystal facet of {001}, {110} and {111} family. The crystal facets of pristine ZIF-8 with methanol solvent are less observed due to the small size of crystals. Possible different crystal shape is observed when ZIF-8 is modulated with NaCl in methanol solvent to give a rhombic dodecahedron crystal shape as shown in Figure 6(h). In this crystal, the dominant crystal facet is indicated to be {110} family. This is corresponding to the X-ray diffraction pattern where lattice family of {110} has relatively significant intensities in all patterns.

3.2 Study of Interaction between ZIF-8 and CO_2

The interaction between CO_2 and ZIF-8 structure has been assessed both using experimental and computational approaches. In this study, ZIF-8 materials were interacted with CO_2 and characterized using an ex-situ approach with IR spectroscopy. Using an ex-situ IR spectroscopy provides prediction in term of the interaction mode that may occur inside the ZIF-8 structure, although it has less information compared to in-situ IR spectroscopy such as using diffuse reflectance IR spectroscopy [39]. The surface area of ZIF-8 material has been reported in previous report indicating relatively large surface area compared to other inorganic materials [40–42]. The presence of NaCl and solvent molecule in this study might affect the surface area, however the interaction between CO_2 and ZIF-8 is still able to be examined using ex-situ IR spectroscopy. In Figure 7, the ex-situ IR spectra are provided for pristine ZIF-8 and ZIF-8 modified with NaCl either in water or methanol solvent.

In general, the IR spectra of ZIF-8 after CO_2 adsorption has no significant difference compared with ZIF-8 prior to CO_2 adsorption. However, possible additional peak occurs for ZIF-8 made in water where a peak at 3623 cm^{-1} presents indicating possible interaction with CO_2. This peak is not presence in ZIF-8 before CO_2 adsorption as shown in Figure 4(a). This peak can be predicted due to the combination of bending (υ_2) and symmetric stretch (υ_3) vibration modes of CO_2 [43]. This peak seems less appearance for ZIF-8 made with methanol solvent in Figure 4(b). Another possible observation is at ~645 cm^{-1} indicating possible bending mode (υ_2) of CO_2 molecule. In addition, peak at 2325 cm^{-1} may also indicate an asymmetric stretch vibration mode of CO_2. The presence of possible solvent molecules either water or methanol may hinder the analysis of CO_2 interaction to ZIF-8. Therefore, further study was conducted using computational approach.

To evaluate the molecular interaction between CO_2 and ZIF-8, a combination of DFT calculation of ZIF-8 cluster and molecular dynamics of periodic ZIF-8 structure containing either water or methanol solvent was performed as shown in Figure 8. According to the DFT calculation, the NaCl location is relatively close to the Zn^{2+} ion with a distance of 3.846 Å and 3.934 Å in the presence of water (Figure 8(a)) and methanol (Figure 8(d)), respectively. Both structures have a preference location of CO_2 molecule to interact with NaCl. CO_2 molecule is relatively close to the Na^+ ion with a dis-

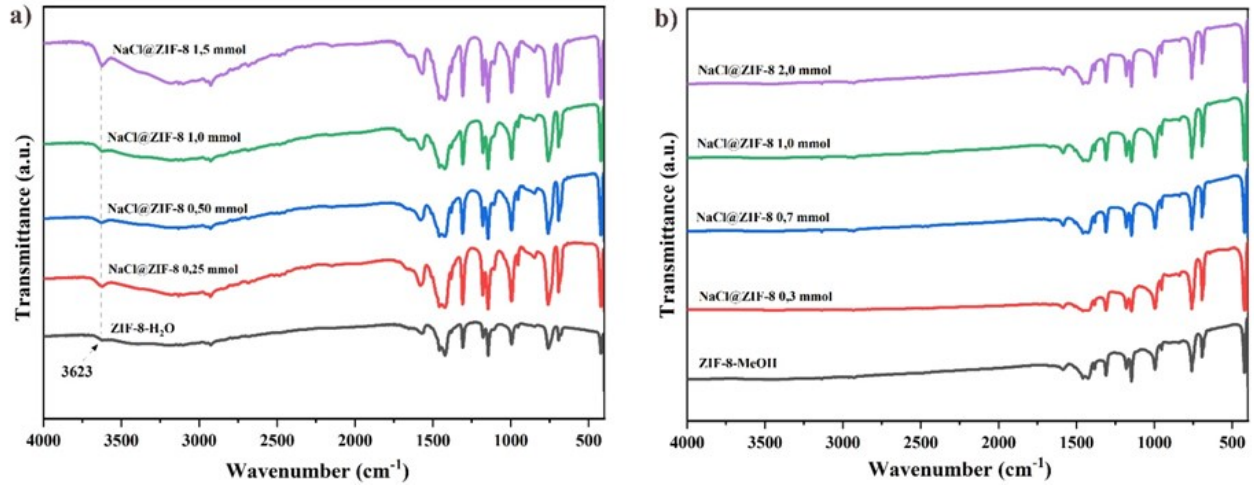

Figure 7. IR spectra of pristine ZIF-8 and ZIF-8 modified with NaCl using H_2O (a) and methanol (b) solvent after interaction with CO_2 gas.

tance of 2.390 and 2.412 Å in the presence of water and methanol, respectively indicating possible stronger intermolecular interaction. Therefore, it results in a low adsorption energy of −0.486 eV and −0.405 eV, for water and methanol solvent based reaction, respectively. The adsorption energy suggests that CO_2 molecule has lower adsorption energy when water is used as the solvent. Additional calculation based on the DFT approach were also conducted where the position of CO_2 molecule is relatively far from the NaCl and resulted in energy

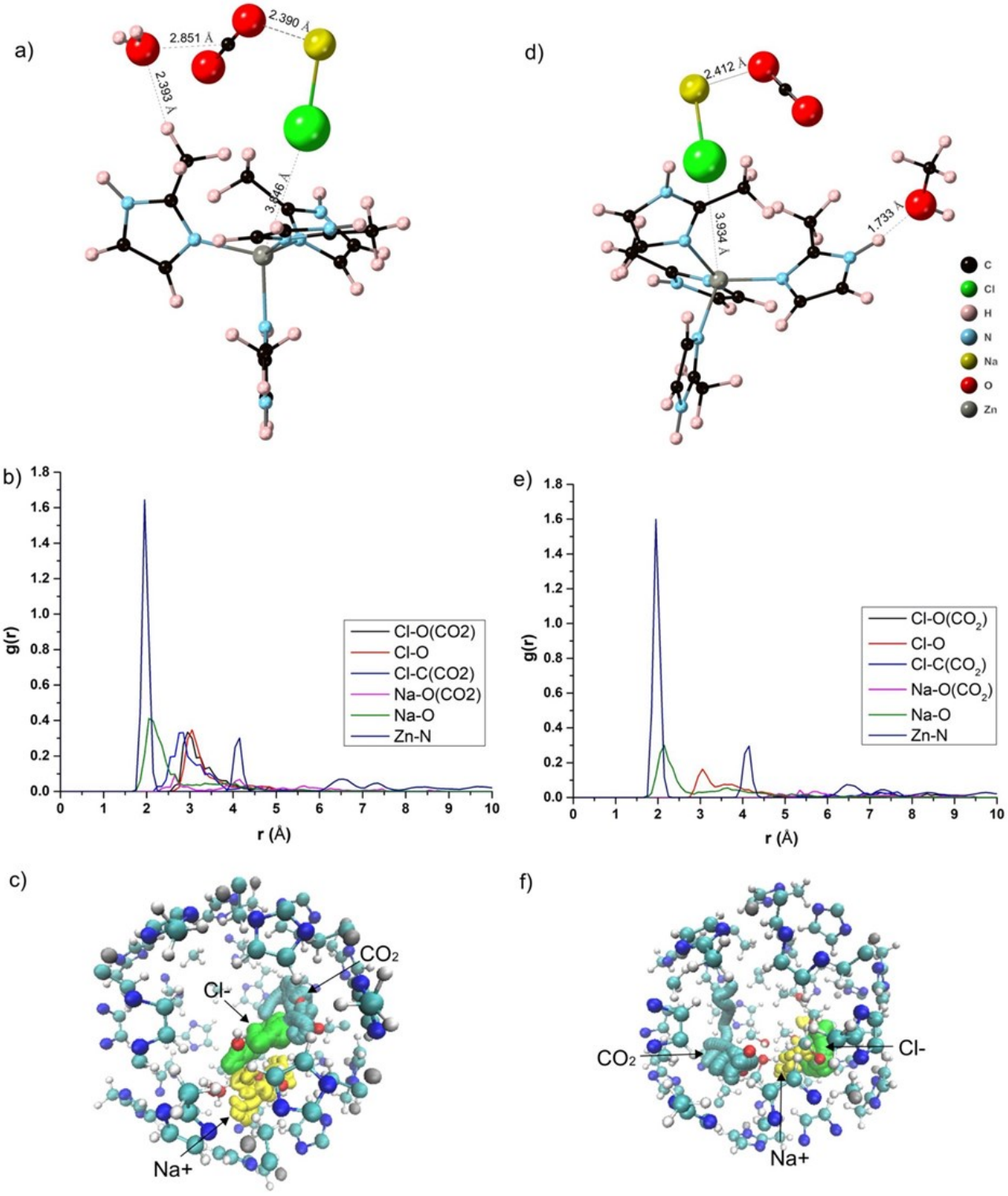

Figure 8. Interaction of CO_2 and ZIF-8 cluster modulated by NaCl in the presence of water (a) and methanol (d) based on DFT calculation. Radial distribution function and trajectory path of CO_2 inside the periodic ZIF-8 structure were also shown in the presence of water (b, c) and methanol (e, f) solvent.

that is relatively higher than when CO_2 is close to the NaCl. This shows that NaCl modulates the properties of ZIF-8 to give additional binding sites for CO_2 molecules.

Molecular dynamics studies based on the GFN2-xTB method were performed for periodic ZIF-8 structure containing 6 molecules of solvent, NaCl and a CO_2 molecule as shown in Figure 8(b,c,e and f). According to the molecular dynamics simulation, the distance of Zn–N maintains about 1.9 – 2.0 Å which is corresponding to the reported value (Figure 8(b,e)). This indicates that during the molecular dynamics simulation, the integrity of the ZIF-8 structure is maintained. Looking at the effect of water and methanol towards CO_2 dynamics, the radial distribution function (RDF) shows an expected behaviour where the radius interaction between Na^+ ion and O atom from either methanol and CO_2 is relatively similar. The Na–O interaction has high probability at the distance of approximately 2.1 Å. This is in correlation with the result from DFT calculation where Na^+ ion is relatively close to the O atom.

The effect of different solvent can be shown from the RDF diagram. In water solvent, six water molecules does not hinder the possible interaction between Na^+ or Cl^- and CO_2 molecule. The RDF shows that various Na^+ to O or Cl^- to O distance is relatively small in distance at the range of 2–4 Å when water is presence as the solvent. However, the presence of methanol seems hinder the possible interaction between Na^+ or Cl^- and CO_2 molecule. In the RDF diagram, the probability of interaction become less as indicated by longer distance more than 3 Å (Figure 8(e)). Additional confirmation was conducted by analysing the trajectory path of CO_2, Na^+ and Cl^- during the molecular dynamics simulation. In Figure 8(c and f), the trajectory of Na^+ and Cl^- is shown with yellow and green colour indicating the mobility of these ions inside the ZIF-8 structure. Their location is identified to be close each other to balance their total ionic charge. The trajectory of CO_2 is shown with the light cyan colour showing the movement of CO_2 molecule inside the ZIF-8 cage. The location of CO_2 is relatively different when water or methanol is present. When six molecules of water are inside the cage, the CO_2 trajectory path seems relatively close to the Na^+ and Cl^- ions. However, when six methanol molecules are presents, there is a gap in trajectory path between CO_2 and Na^+ or Cl^- ions as shown in Figure 8(f). This can be explained due to the difference in molecular size of the solvent. Methanol has relatively larger molecular size than water molecule. Therefore, methanol provides a well separate region between CO_2 and NaCl. This is in relation to the DFT calculation that the adsorption energy of CO_2 is lower when water is presence inside the ZIF-8 cage compared to when methanol is used.

4. Conclusion

The synthesis of ZIF-8 has been conducted in the presence of NaCl as modulation agent. The synthesis was performed using different solvents of either water or methanol solvent. The ZIF-8 materials show no significant structural changes as identified with X-ray diffraction pattern when NaCl is present during the in-situ synthesis. The ZIF-8 material modulated with NaCl shows an average lattice parameter which is reasonably close to the reported ZIF-8 lattice dimension. Due to small difference in lattice parameters in all ZIF-8 modulated with NaCl, it is predicted that NaCl resides inside the ZIF-8 cage without possible ion exchange with Zn^{2+}. Further DFT calculation prove the preferable location of NaCl close to the ZIF-8 tetrahedral cluster. The formation of ZIF-8 structure was confirmed by IR spectra due to the presence of stretching vibration mode of Zn–N at 421 cm^{-1}. The crystal morphology of ZIF-8 modulated with NaCl seem to have different nature, where synthesis using methanol as the solvent gives crystal shape of truncated cubic as well as rhombic dodecahedron. ZIF-8 synthesised with water shows a relatively spherical crystal or particle shape. The effect of solvent molecules has been examined for the adsorption of CO_2 gas. A combination of ex-situ IR spectroscopy and modelling predict possible molecular vibrations as well as binding mode of CO_2 molecules. It is generally concluded that the presence of NaCl provides additional binding sites for CO_2 molecules. This study gives a deeper understanding of the nature of ZIF-8 synthesis in the presence of NaCl with various solvents and its potential for gas capture.

Acknowledgements

Authors greatly thank to the *Final Project Recognition Grant* Universitas Gadjah Mada *Number* 5075/UN1.P.II/Dit-Lit/PT.01.01/2023

CRediT Author Statement

Author contribution: *L. Priandani*: Validation, formal analysis, investigation, visualization, writing: review and editing; *A. Aliefa*: Validation, formal analysis, investigation, visuali-

zation, writing: review and editing; *O. P. Arjasa*: Validation, investigation, resources, writing: review and editing; *F. I. Pambudi*: Conceptualization, validation, data curation, writing: original draft, supervision, funding acquisition. All authors have read and agreed to the published version of the manuscript.

References

[1] Friedlingstein, P., Houghton, R.A., Marland, G., Hackler, J., Boden, T.A., Conway, T.J., Canadell, J.G., Raupach, M.R., Ciais, P., Le Quéré, C. (2010). Update on CO_2 emissions. *Nature Geoscience*, 3, 811–812. DOI: 10.1038/ngeo1022.

[2] Zoundi, Z. (2017). CO2 emissions, renewable energy and the Environmental Kuznets Curve, a panel cointegration approach. *Renewable and Sustainable Energy Reviews*, 72, 1067–1075. DOI: 10.1016/j.rser.2016.10.018.

[3] Yu, K.M.K., Curcic, I., Gabriel, J., Tsang, S.C.E. (2008). Recent Advances in CO_2 Capture and Utilization, *ChemSusChem*, 1, 893–899. DOI: 10.1002/cssc.200800169.

[4] Mac Dowell, N., Fennell, P.S., Shah, N., Maitland, G.C. (2017). The role of CO2 capture and utilization in mitigating climate change. *Nature Climate Change*, 7, 243–249. DOI: 10.1038/nclimate3231.

[5] He, H., Perman, J.A., Zhu, G., Ma, S. (2016). Metal-Organic Frameworks for CO_2 Chemical Transformations. *Small*, 12, 6309–6324. DOI: 10.1002/smll.201602711.

[6] Daiyan, R., Zhu, X., Tong, Z., Gong, L., Razmjou, A., Liu, R.-S., Xia, Z., Lu, X., Dai, L., Amal, R. (2020). Transforming active sites in nickel–nitrogen–carbon catalysts for efficient electrochemical CO_2 reduction to CO. *Nano Energy*, 78, 105213. DOI: 10.1016/j.nanoen.2020.105213.

[7] Kondratenko, E.V., Mul, G., Baltrusaitis, J., Larrazábal, G.O., Pérez-Ramírez, J. (2013). Status and perspectives of CO_2 conversion into fuels and chemicals by catalytic, photocatalytic and electrocatalytic processes. *Energy & Environmental Science*, 6, 3112. DOI: 10.1039/c3ee41272e.

[8] Ding, M., Flaig, R.W., Jiang, H.-L., Yaghi, O.M. (2019). Carbon capture and conversion using metal–organic frameworks and MOF-based materials. *Chemical Society Reviews*, 48, 2783–2828. DOI: 10.1039/C8CS00829A.

[9] Choe, J.H., Kim, H., Hong, C.S. (2021). MOF-74 type variants for CO_2 capture. *Materials Chemistry Frontiers*, 5, 5172–5185. DOI: 10.1039/D1QM00205H.

[10] Hu, Z., Wang, Y., Shah, B.B., Zhao, D. (2019). CO_2 Capture in Metal-Organic Framework Adsorbents: An Engineering Perspective. *Advanced Sustainable Systems*, 3, 1800080. DOI: 10.1002/adsu.201800080.

[11] Freund, R., Zaremba, O., Arnauts, G., Ameloot, R., Skorupskii, G., Dincă, M., Bavykina, A., Gascon, J., Ejsmont, A., Goscianska, J., Kalmutzki, M., Lächelt, U., Ploetz, E., Diercks, C.S., Wuttke, S. (2021). The Current Status of MOF and COF Applications. *Angewandte Chemie International Edition*, 60, 23975–24001. DOI: 10.1002/anie.202106259.

[12] Wang, Q., Astruc, D. (2020). State of the Art and Prospects in Metal–Organic Framework (MOF)-Based and MOF-Derived Nanocatalysis. *Chemical Reviews*, 120, 1438–1511. DOI: 10.1021/acs.chemrev.9b00223.

[13] Ghanbari, T., Abnisa, F., Wan Daud, W.M.A. (2020). A review on production of metal organic frameworks (MOF) for CO2 adsorption. *Science of The Total Environment*, 707, 135090. DOI:10.1016/j.scitotenv.2019.135090.

[14] Loiseau, T., Lecroq, L., Volkringer, C., Marrot, J., Férey, G., Haouas, M., Taulelle, F., Bourrelly, S., Llewellyn, P.L., Latroche, M. (2006). MIL-96, a Porous Aluminum Trimesate 3D Structure Constructed from a Hexagonal Network of 18-Membered Rings and μ_3-Oxo-Centered Trinuclear Units. *Journal of the American Chemical Society*, 128, 10223–10230. DOI: 10.1021/ja0621086.

[15] Surblé, S., Millange, F., Serre, C., Düren, T., Latroche, M., Bourrelly, S., Llewellyn, P.L., Férey, G. (2006). Synthesis of MIL-102, a Chromium Carboxylate Metal−Organic Framework, with Gas Sorption Analysis. *Journal of the American Chemical Society*, 128, 14889–14896. DOI: 10.1021/ja064343u.

[16] Wang, B., Côté, A.P., Furukawa, H., O'Keeffe, M., Yaghi, O.M. (2008). Colossal cages in zeolitic imidazolate frameworks as selective carbon dioxide reservoirs. *Nature*, 453, 207–211. DOI: 10.1038/nature06900.

[17] Bae, Y.-S., Mulfort, K.L., Frost, H., Ryan, P., Punnathanam, S., Broadbelt, L.J., Hupp, J.T., Snurr, R.Q. (2008). Separation of CO_2 from CH_4 Using Mixed-Ligand Metal−Organic Frameworks. *Langmuir*, 24, 8592–8598. DOI: 10.1021/la800555x.

[18] Xue, M., Ma, S., Jin, Z., Schaffino, R.M., Zhu, G.-S., Lobkovsky, E.B., Qiu, S.-L., Chen, B. (2008). Robust Metal−Organic Framework Enforced by Triple-Framework Interpenetration Exhibiting High H_2 Storage Density. *Inorganic Chemistry*, 47, 6825–6828. DOI: 10.1021/ic800854y.

[19] Llewellyn, P.L., Bourrelly, S., Serre, C., Filinchuk, Y., Férey, G. (2006). How Hydration Drastically Improves Adsorption Selectivity for CO_2 over CH_4 in the Flexible Chromium Terephthalate MIL-53. *Angewandte Chemie International Edition*, 45, 7751–7754. DOI: 10.1002/anie.200602278.

[20] Ma, S., Wang, X.-S., Manis, E.S., Collier, C.D., Zhou, H.-C. (2007). Metal−Organic Framework Based on a Trinickel Secondary Building Unit Exhibiting Gas-Sorption Hysteresis. *Inorganic Chemistry*, 46, 3432–3434. DOI: 10.1021/ic070338v.

[21] Hayashi, H., Côté, A.P., Furukawa, H., O'Keeffe, M., Yaghi, O.M. (2007). Zeolite A imidazolate frameworks. *Nature Materials*, 6, 501–506. DOI: 10.1038/nmat1927.

[22] Cho, J.H., Lee, C., Hong, S.H., Jang, H.Y., Back, S., Seo, M., Lee, M., Min, H., Choi, Y., Jang, Y.J., Ahn, S.H., Jang, H.W., Kim, S.Y. (2022). Transition Metal Ion Doping on ZIF-8 Enhances the Electrochemical CO_2 Reduction Reaction. *Advanced Materials*, 2022, 2208224. DOI: 10.1002/adma.202208224.

[23] Sun, J., Semenchenko, L., Lim, W.T., Ballesteros Rivas, M.F., Varela-Guerrero, V., Jeong, H.K. (2018). Facile synthesis of Cd-substituted zeolitic-imidazolate framework Cd-ZIF-8 and mixed-metal CdZn-ZIF-8. *Microporous and Mesoporous Materials*, 264, 35–42. DOI: 10.1016/j.micromeso.2017.12.032.

[24] Zaręba, J.K., Nyk, M., Samoć, M. (2016). Co/ZIF-8 Heterometallic Nanoparticles: Control of Nanocrystal Size and Properties by a Mixed-Metal Approach. *Crystal Growth & Design*, 16, 6419–6425. DOI: 10.1021/acs.cgd.6b01090.

[25] Ding, R., Zheng, W., Yang, K., Dai, Y., Ruan, X., Yan, X., He, G. (2020). Amino-functional ZIF-8 nanocrystals by microemulsion based mixed linker strategy and the enhanced CO_2/N_2 separation. *Separation and Purification Technology*, 236, 116209. DOI: 10.1016/j.seppur.2019.116209.

[26] Park, S., Jeong, H.-K. (2020). In-situ linker doping as an effective means to tune zeolitic-imidazolate framework-8 (ZIF-8) fillers in mixed-matrix membranes for propylene/propane separation. *Journal of Membrane Science*, 596, 117689. DOI: 10.1016/j.memsci.2019.117689.

[27] Pan, Y., Heryadi, D., Zhou, F., Zhao, L., Lestari, G., Su, H., Lai, Z. (2011). Tuning the crystal morphology and size of zeolitic imidazolate framework-8 in aqueous solution by surfactants. *CrystEngComm*, 13, 6937. DOI: 10.1039/c1ce05780d.

[28] Wang, S., Lv, Y., Yao, Y., Yu, H., Lu, G. (2018). Modulated synthesis of monodisperse MOF-5 crystals with tunable sizes and shapes. *Inorganic Chemistry Communications*, 93, 56–60. DOI: 10.1016/j.inoche.2018.05.010.

[29] Cho, W., Lee, H.J., Oh, M. (2008). Growth-Controlled Formation of Porous Coordination Polymer Particles. *Journal of the American Chemical Society*, 130, 16943–16946. DOI: 10.1021/ja8039794.

[30] Pang, M., Cairns, A.J., Liu, Y., Belmabkhout, Y., Zeng, H.C., Eddaoudi, M. (2012). Highly Monodisperse M^{III} -Based soc-MOFs (M = In and Ga) with Cubic and Truncated Cubic Morphologies. *Journal of the American Chemical Society*, 134, 13176–13179. DOI: 10.1021/ja3049282.

[31] Abdelhamid, H.N. (2020). Salts Induced Formation of Hierarchical Porous ZIF-8 and Their Applications for CO_2 Sorption and Hydrogen Generation via $NaBH_4$ Hydrolysis. Macromolecular Chemistry and Physics, 221, 2000031. DOI: 10.1002/macp.202000031.

[32] Neese, F. (2012). The ORCA program system. *WIREs Computational Molecular Science*, 2, 73–78. https://doi.org/10.1002/WCMS.81.

[33] Pambudi, F.I. (2022). Electronic properties of heterometallic zeolitic imidazolate framework and its encapsulation with Ni, Pd and Pt. Inorganic Chemistry Communications, 143, 109798. DOI: 10.1016/j.inoche.2022.109798.

[34] Perdew, J.P., Burke, K., Ernzerhof, M. (1996). Generalized gradient approximation made simple. *Physical Review Letters*, 77, 3865–3868. DOI: 10.1103/PhysRevLett.77.3865.

[35] Grimme, S., Ehrlich, S., Goerigk, L. (2011). Effect of the damping function in dispersion corrected density functional theory. *Journal of Computational Chemistry*, 32, 1456–1465. DOI: 10.1002/jcc.21759.

[36] Bannwarth, C., Ehlert, S., Grimme, S. (2019). GFN2-xTB—An Accurate and Broadly Parametrized Self-Consistent Tight-Binding Quantum Chemical Method with Multipole Electrostatics and Density-Dependent Dispersion Contributions. *Journal of Chemical Theory and Computation*, 15, 1652–1671. DOI: 10.1021/acs.jctc.8b01176.

[37] Hourahine, B., Aradi, B., Blum, V., Bonafé, F., Buccheri, A., Camacho, C., Cevallos, C., Deshaye, M.Y., Dumitrică, T., Dominguez, A., Ehlert, S., Elstner, M., van der Heide, T., Hermann, J., Irle, S., Kranz, J.J., Köhler, C., Kowalczyk, T., Kubař, T., Lee, I.S., Lutsker, V., Maurer, R.J., Min, S.K., Mitchell, I., Negre, C., Niehaus, T.A., Niklasson, A.M.N., Page, A.J., Pecchia, A., Penazzi, G., Persson, M.P., Řezáč, J., Sánchez, C.G., Sternberg, M., Stöhr, M., Stuckenberg, F., Tkatchenko, A., Yu, V.W.-z., Frauenheim, T. (2020). DFTB+, a software package for efficient approximate density functional theory based atomistic simulations. *The Journal of Chemical Physics*, 152, 124101. DOI: 10.1063/1.5143190.

[38] Park, K.S., Ni, Z., Côté, A.P., Choi, J.Y., Huang, R., Uribe-Romo, F.J., Chae, H.K., O'Keeffe, M., Yaghi, O.M. (2006). Exceptional chemical and thermal stability of zeolitic imidazolate frameworks. *Proceedings of the National Academy of Sciences*, 103, 10186–10191. DOI: 10.1073/pnas.0602439103.

[39] Hadjiivanov, K.I., Panayotov, D.A., Mihaylov, M.Y., Ivanova, E.Z., Chakarova, K.K., Andonova, S.M., Drenchev, N.L. (2021). Power of Infrared and Raman Spectroscopies to Characterize Metal-Organic Frameworks and Investigate Their Interaction with Guest Molecules. *Chemical Reviews*, 121, 1286–1424. DOI: 10.1021/acs.chemrev.0c00487.

[40] Mohammadi, A., Nakhaei Pour, A. (2023). Triethylenetetramine-impregnated ZIF-8 nanoparticles for CO_2 adsorption. *Journal of CO2 Utilization*, 69, 102424. DOI: 10.1016/j.jcou.2023.102424.

[41] Pokhrel, J., Bhoria, N., Anastasiou, S., Tsoufis, T., Gournis, D., Romanos, G., Karanikolos, G.N. (2018). CO2 adsorption behavior of amine-functionalized ZIF-8, graphene oxide, and ZIF-8/graphene oxide composites under dry and wet conditions. *Microporous and Mesoporous Materials*, 267, 53–67. DOI: 10.1016/j.micromeso.2018.03.012.

[42] Zhang, Z., Xian, S., Xi, H., Wang, H., Li, Z. (2011). Improvement of CO2 adsorption on ZIF-8 crystals modified by enhancing basicity of surface. *Chemical Engineering Science*, 66, 4878–4888. DOI: 10.1016/j.ces.2011.06.051.

[43] Hu, Y., Liu, Z., Xu, J., Huang, Y., Song, Y. (2013). Evidence of Pressure Enhanced CO_2 Storage in ZIF-8 Probed by FTIR Spectroscopy. *Journal of the American Chemical Society,* 135, 9287–9290. DOI: 10.1021/ja403635b.

Bulletin of Chemical Reaction Engineering & Catalysis, 18 (3), 2023, 536

Supporting Information for DOI: 10.9767/bcrec.20033

An Experimental and Computational Study of Zeolitic Imidazolate Framework (ZIF-8) Synthesis Modulated with Sodium Chloride and Its Interaction with CO_2

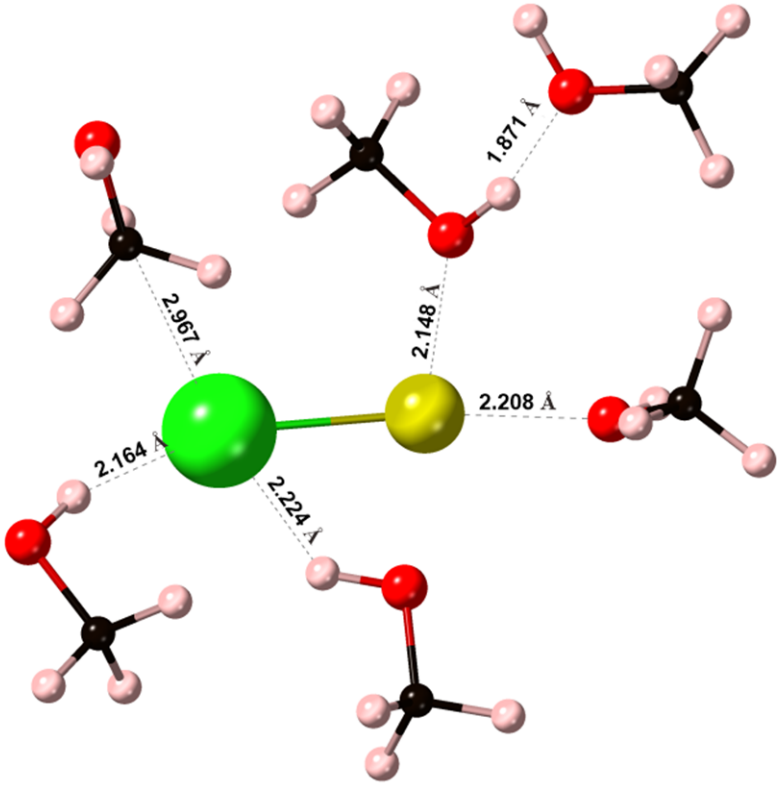

Figure S1. Methanol cluster inside ZIF-8 cages in the presence of NaCl. The ZIF-8 structure is omitted to give better view of the methanol cluster. Na, Cl, C, O and H are coloured yellow, green, black, red, and pink, respectively. .

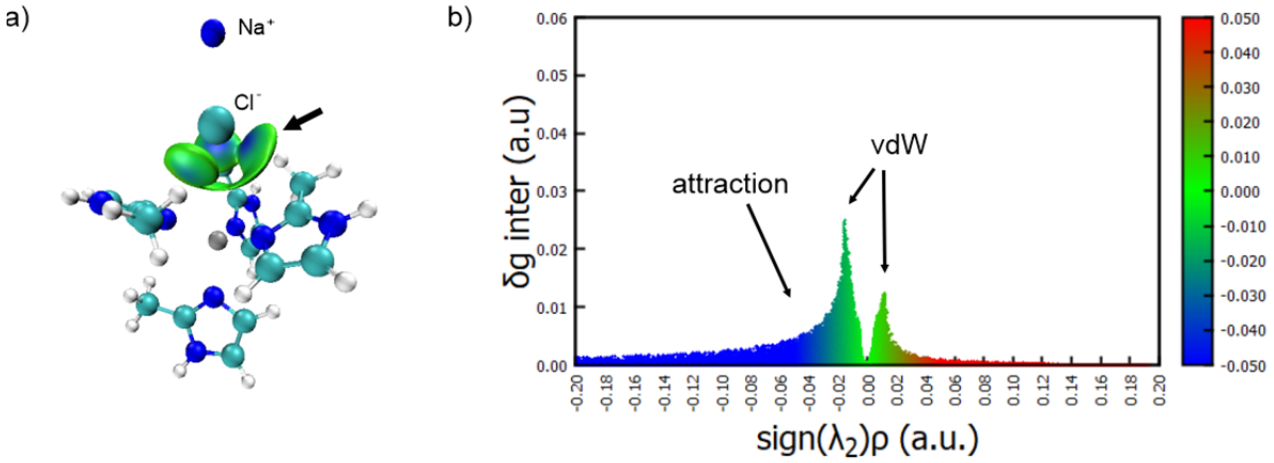

Figure S2. Interaction between NaCl and ZIF-8 shown as an isosurface structure (a) and independent gradient maps (b) indicating possible intermolecular interactions.

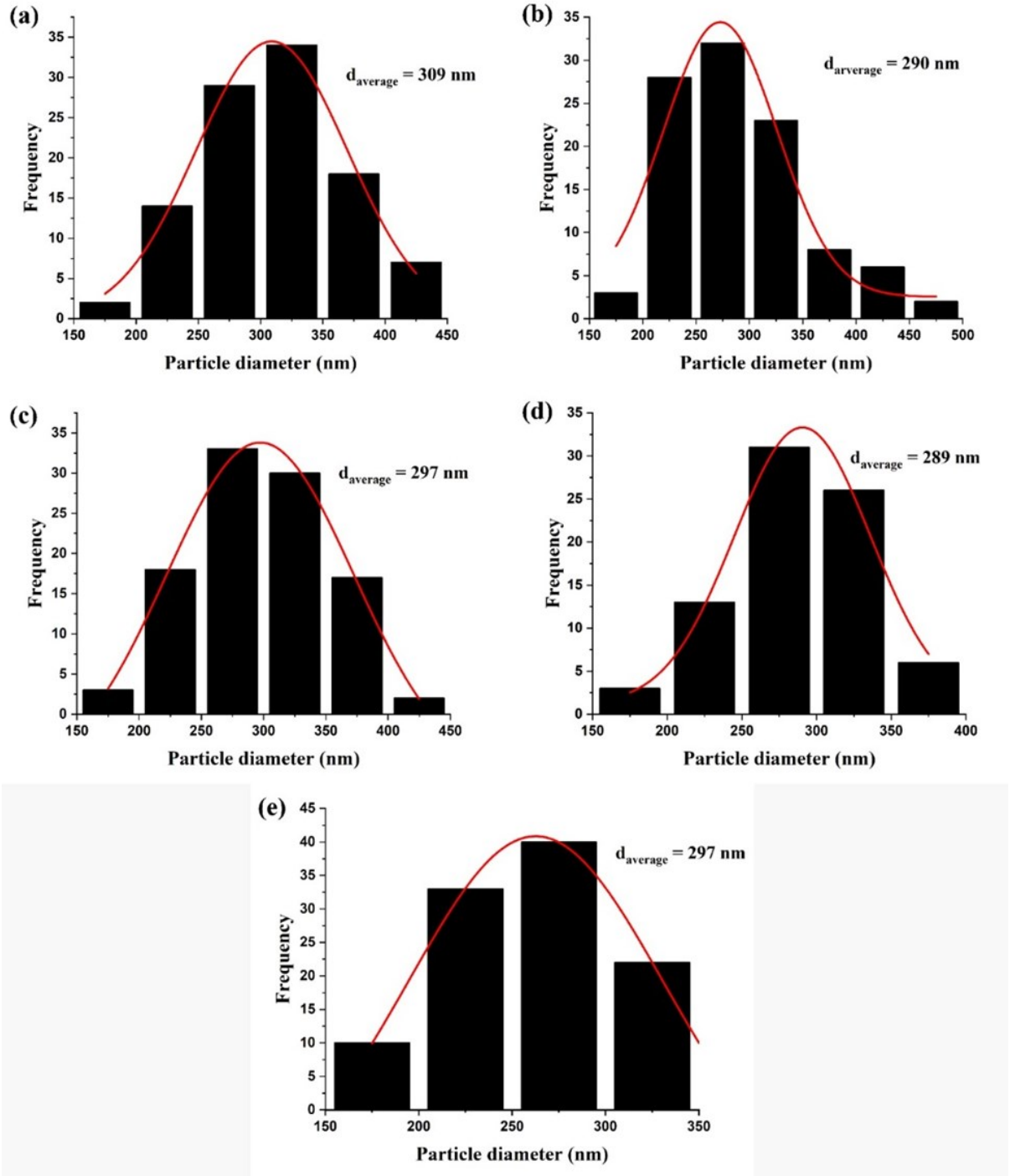

Figure S3. Distribution of particle size of pristine ZIF-8 and ZIF-8 modulated with NaCl in water solvent

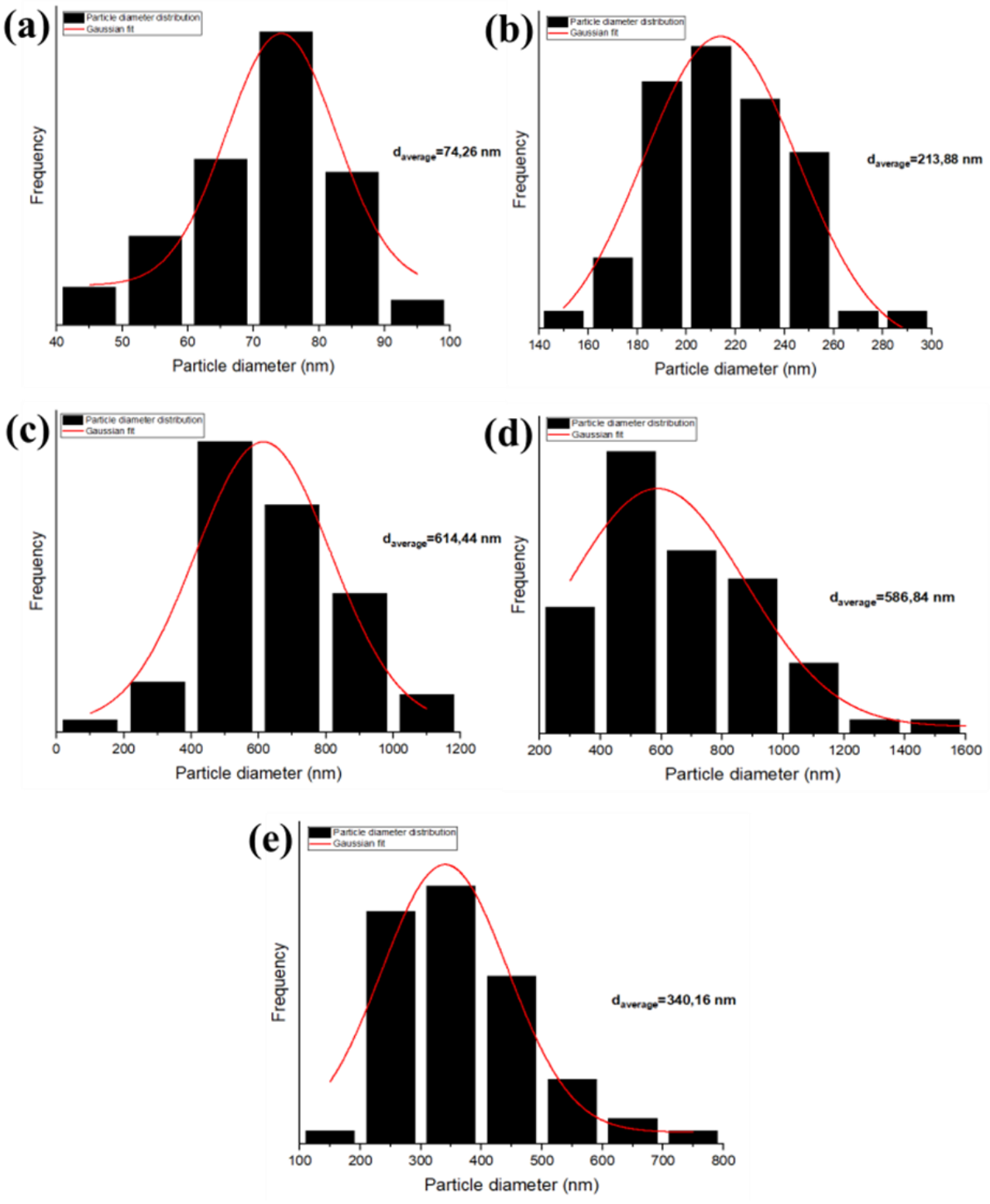

Figure S4. Distribution of particle size of pristine ZIF-8 and ZIF-8 modulated with NaCl in methanol solvent